

Structure of Possible Long-lived Asteroid Belts

N.W. Evans¹ and S.A. Tabachnik²,

¹ *Theoretical Physics, 1 Keble Road, Oxford OX1 3NP*

² *Princeton University Observatory, Peyton Hall, Princeton, NJ 08544-1001, USA*

Received ...; accepted ...

ABSTRACT

High resolution simulations are used to map out the detailed structure of two long-lived stable belts of asteroid orbits in the inner Solar system. The Vulcanoid belt extends from 0.09 to 0.20 astronomical units (au), though with a gaps at 0.15 and 0.18 au corresponding to de-stabilising mean motion resonances with Mercury and Venus. As collisional evolution proceeds slower at larger heliocentric distances, kilometre-sized or larger Vulcanoids are most likely to be found in the region between 0.16 and 0.18 au. The optimum location in which to search for Vulcanoids is at geocentric ecliptic longitudes $9^\circ \leq |\ell_g| \leq 10^\circ$ and latitudes $|\beta_g| < 1^\circ$. Dynamically speaking, the Earth-Mars belt between 1.08–1.28 au is an extremely stable repository for asteroids on nearly circular orbits. It is interrupted at 1.21 au due to the 3:4 commensurability with the Earth, while secular resonances with Saturn are troublesome beyond 1.17 au. These detailed maps of the fine structure of the belts can be used to plan search methodologies. Strategies for detecting members of the belts are discussed, including the use of infrared wide-field imaging with VISTA, and forthcoming European Space Agency satellite missions like *GAIA* and *BepiColombo*.

Key words: Solar system: general – minor planets, asteroids – planets and satellites: Mercury, the Earth, Mars

1 INTRODUCTION

The most abundant minor bodies of the Solar system are the asteroids whose Main Belt extends between 2 and 3.5 au. The asteroids are remnant planetesimals. It has often been suggested that the Main Belt is perhaps the only zone in the Solar System where planetesimals can survive in long-lived orbits for ages of the order of 4.5 Gyrs (e.g., Chapman 1987; Laskar 1997). Recently, however, Holman (1997) uncovered evidence for a possible belt between Uranus and Neptune by 4.5 Gyr integrations of test particles in the gravity field of the Sun and the four massive planets. Mikkola & Innanen (1995) performed a 3 Myr test particle calculation in the inner Solar system which suggested the existence of narrow bands of stability between each of the terrestrial planets. Subsequently, Evans & Tabachnik (1999) reported the results of 100 Myr test particle calculations. Extrapolating the results to the age of the Solar system, they conjectured that there might be two long-lived belts of stable asteroids in the inner Solar system. These are the domain of the Vulcanoids between 0.09 and 0.20 astronomical units (au) and the Earth-Mars belt between 1.08 and 1.28 au respectively.

In this *Letter*, we report results on the structure of the belts inferred from high resolution numerical simulations. The general procedure is similar to many recent studies on the stability of test particles in the Solar system. At semima-

ior axes separated by 0.002 au in each of the two belts, five test particles are launched on initially circular orbits in the ecliptic with starting longitudes $n \times 72^\circ$ with $n = 0, \dots, 4$. The test particles are perturbed by the Sun and planets, but do not themselves exert any gravitational forces. The full effects of all the planets (except Pluto) are included. The initial positions and velocities of the planets, as well as their masses, come from the JPL Planetary and Lunar Ephemerides DE405 and the starting epoch is JD 2440400.5 (28 June 1969). After each timestep, the test particles are examined. If their orbits have become hyperbolic, or if they have entered the sphere of influence of any planet or if they have approached closer than ten solar radii to the Sun, then they are removed. The simulations are run for 100 Myr. The calculations for the 300 Vulcanoid test particles are performed in long double precision to minimise round-off error. The 500 test particles in the Earth-Mars belt are simulated using double precision on the Oxford Supercomputer. Even using a fast symplectic integrator with individual timesteps (Saha & Tremaine 1994), the calculations still consumed several months.

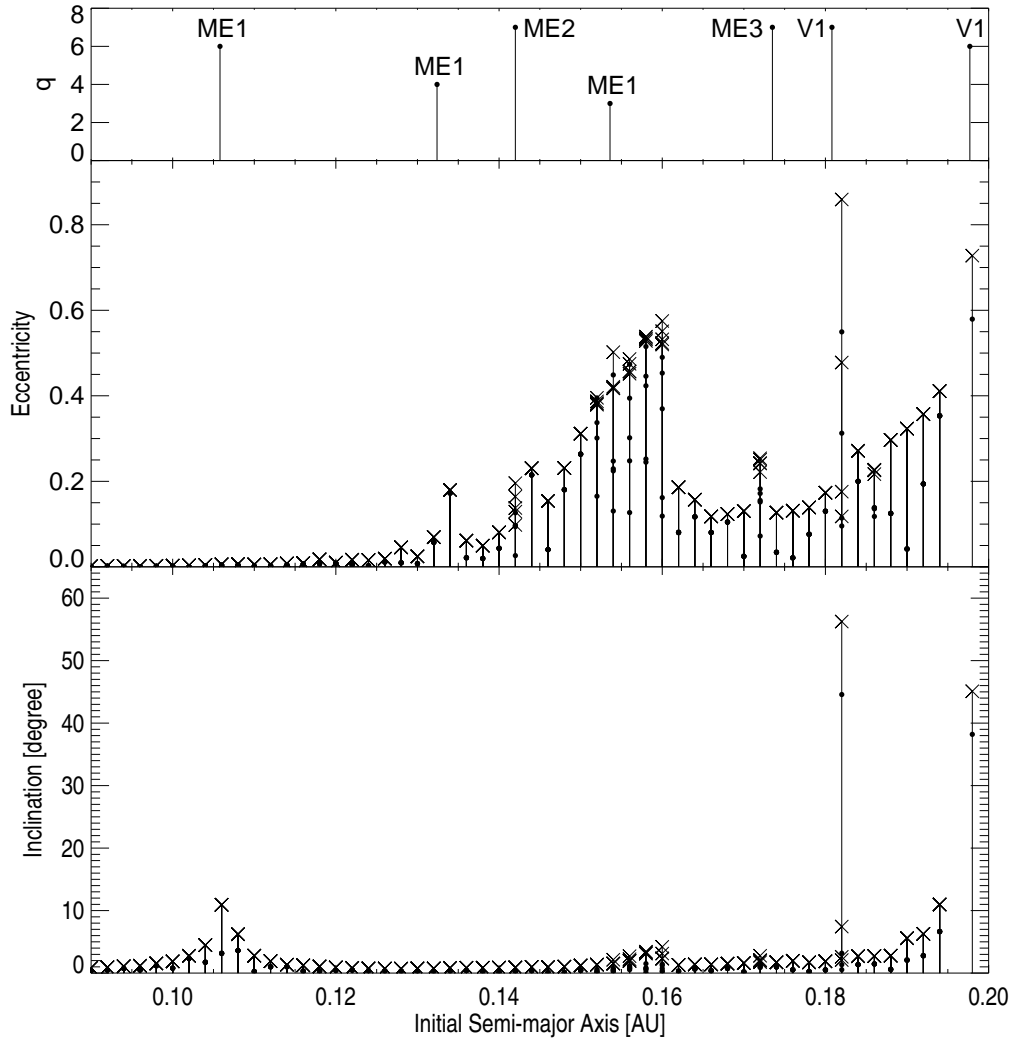


Figure 1. The two lower panels show the eccentricity and the inclination of the remaining test particles in the Vulcanoid belt after 100 Myr. Filled circles represent the instantaneous values, while crosses indicate the maximum values over the integration timespan. The location of the mean motion resonances are plotted in the topmost panel according to the order of the commensurability q . The notation ME and V refers to Mercury and Venus respectively, while the number following it is the value of k in equation (1).

2 THE VULCANOIDS

The Vulcanoids are a population of intra-Mercurial bodies originally proposed by Weidenschilling (1978) to resolve seeming contradictions in the geological and cratering history of Mercury. The inner edge of the Vulcanoid belt is ~ 0.09 au. Small bodies closer than this to the Sun are removed as a consequence of both Poynting-Robertson drag and the Yarkovsky effect (e.g., Vokroulický, Farinella & Bottke 2000). Evans & Tabachnik (1999) argued that the outer edge is 0.20 au. Small bodies closer than this to Mercury evolve swiftly into the planet's sphere of influence. The robustness of orbits in the Vulcanoid belt stems from the fact that there is only one bounding planet and so it is analogous to the stability of the Kuiper-Edgeworth belt. Even after 100 Myr, some 80% of the Vulcanoid orbits still have eccentricities $e < 0.2$ and inclinations $i < 10^\circ$ in our high resolution simulation. The two lower panels of Figure 1 illustrate the eccentricities and inclinations of the surviving test particles at the end of the integration. In the interval $0.09 \leq a_{\text{tp}} \leq 0.20$, the averaged values for the eccentricity

are $\langle e_{\text{inst}} \rangle = 0.0935$ and $\langle e_{\text{max}} \rangle = 0.15$ and for the inclination $\langle i_{\text{inst}} \rangle = 1.21^\circ$ and $\langle i_{\text{max}} \rangle = 5.36^\circ$, the subscripts referring to the instantaneous and maximum quantities respectively. The upper panel indicates the location of the mean motion resonances, which occur when the orbital period of one planet $n_p \sim a_p^{-3/2}$ and a test particle $n_{\text{tp}} \sim a_{\text{tp}}^{-3/2}$ are commensurable, or close to the ratio of small integers

$$\frac{n_{\text{tp}}}{n_p} = \begin{cases} \frac{k+q}{k} & \text{if } a_{\text{tp}} < a_p, \\ \frac{k}{k+q} & \text{if } a_{\text{tp}} > a_p. \end{cases} \quad (1)$$

Here, a_{tp} and a_p are the semimajor axes of the test particle and the planet respectively. From classical perturbation theory, the strength of the resonance is roughly indicated by the order of the commensurability q . On the uppermost panel of Figure 1, each resonance is labelled according to the planet and the number k . For example, the resonance ME2 at semimajor axis $a_{\text{tp}} = 0.142$ au with $q = 7$ corresponds to a mean motion ration of $9/2$ with Mercury. As seen from the Figure, some resonances tend to excite the

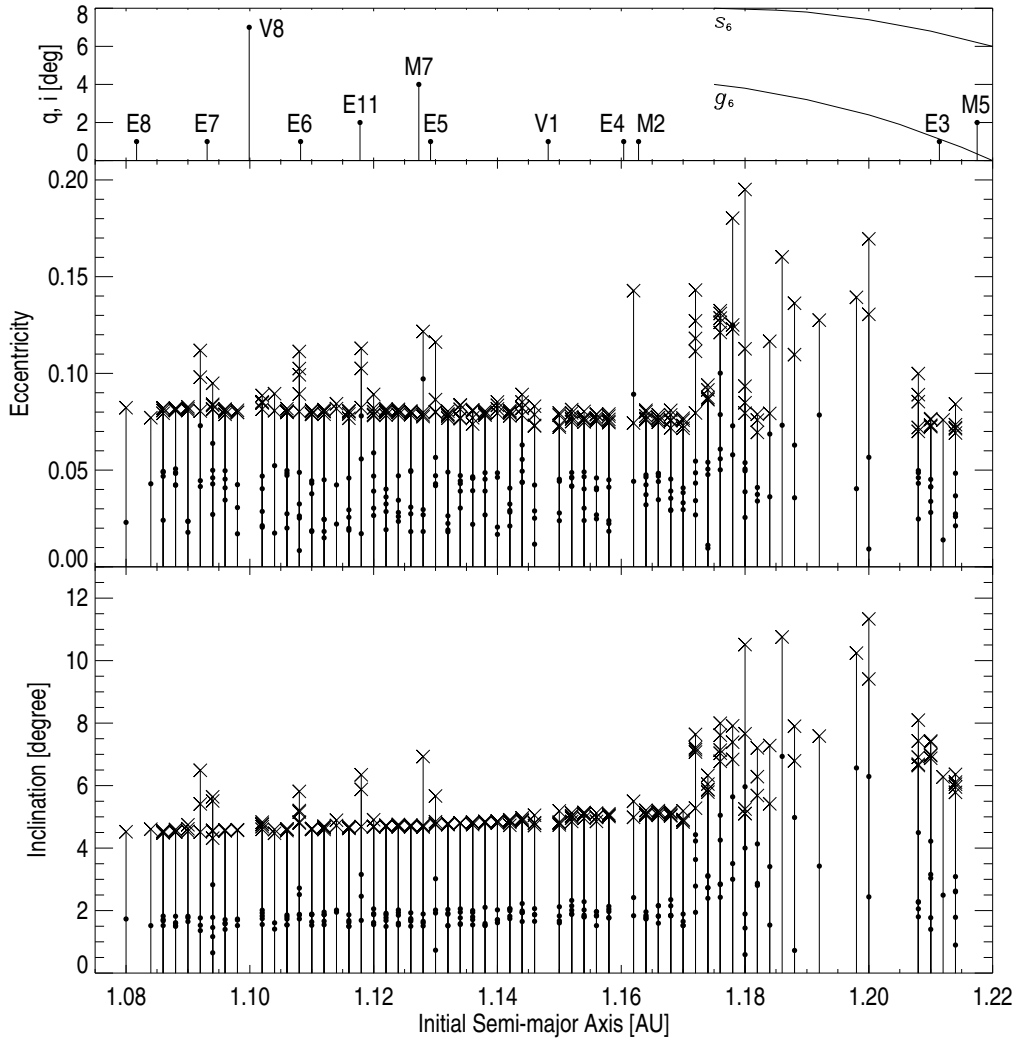


Figure 2. The two lower panels illustrate the eccentricity and the inclination of the remaining test particles in the Earth-Mars belt after 100 Myr. Again, filled circles and crosses represent the instantaneous and the maximum values. The upper panel shows the location of the mean motion and secular resonances. The notation V, E and M refers to Venus, the Earth and Mars. From 1.175 au to 1.22 au, the two arcs labelled g_6 and s_6 mark the locations at which two linear secular resonances due to Saturn are prominent as a function of semimajor axis and inclination. We note that the stable region between 1.208 and 1.214 au is interrupted at 1.212 au due to the 3:4 commensurability with the Earth.

test particle's inclination (ME1, $q = 6$), while others pump up the eccentricity (ME1, $q = 4$; ME2, $q = 7$; ME1, $q = 3$; ME3, $q = 7$). The effect of the Mercurian resonances occurs over a relatively broad span of semimajor axes, (especially near ME1, $q = 3$) probably because of the wide range of eccentricity ($0.1 < e < 0.3$) and inclination ($0^\circ < i < 10.5^\circ$) that Mercury undergoes over the 100 Myr integration timespan. Conversely, the effects of the Venusian resonances (V1, $q = 7$; V1, $q = 6$) appear much more localized at semimajor axes 0.181 au and 0.198 au and excite both the eccentricity and the inclination of the test particle.

The collisional time scale in the Vulcanoid belt is short because the volume of space is small and because the relative velocities are high. Any sizeable population of bodies must have evolved through mutual collisions. Numerical models of the collisional processes (Stern & Durda 2000) suggest that a population of at most a few hundred objects with radii larger than 1 km could have survived from primordial times. As collisional evolution proceeds most quickly at

smaller heliocentric distances, Stern & Durda suggest that the most favourable location to search is nearly circular orbits near the very outer edge of the dynamical stable Vulcanoid belt (~ 0.2 au). However, Figure 1 shows that the Venusian resonance (V1, $q = 6$) at 0.198 au excites both the eccentricity and inclination of such objects. Rather, it is the region slightly inward between 0.16 and 0.18 au that is the most likely to contain surviving objects. In other words, the optimum location in which to search for Vulcanoids is $9^\circ \lesssim |\ell_g| \lesssim 10^\circ$ and $|\beta_g| \lesssim 1^\circ$, where (ℓ_g, β_g) are geocentric ecliptic longitude and latitude.

Very recently, two searches using the Large Angle Spectroscopic Coronagraph (LASCO) on the *SOHO* satellite have been conducted (Durda et al. 2000; Schumacher & Gay 2001). In particular, Durda et al. found no Vulcanoids to a moving object detection limiting magnitude of $V \sim 8$, corresponding to objects ~ 50 km in diameter. There have also been a number of daytime searches with infrared telescopes (Leake et al. 1987; Campins et al. 1996), although limited

to small fields of view. The closeness of Vulcanoids to the Sun causes them to be hot. The search strategy exploits the fact that Vulcanoids have a substantial component of infrared emission with the K and L bands offering the best chances of detection. Leake et al. reached a limiting magnitude of $L \sim 5$ but covered only ~ 6 square degrees of the sky. The new infrared wide-field telescope VISTA ^{*} has a field of view of 0.5 square degrees in the K band and will be ideal for deep Vulcanoid searches in the ecliptic centered around $9^\circ \lesssim |\ell_g| \lesssim 10^\circ$.

The European Space Agency (ESA) satellite *Bepi-Colombo* [†] is scheduled for launch in 2009. Its main objective is to orbit and image the planet Mercury. However, it will also be equipped with a small telescope (20-30cm) and CCD camera for asteroid detection. The telescope points in the direction of motion of the satellite, which is in a polar orbit around the planet. Since the satellite is continuously looking at the surface of Mercury, the telescope is rotating with respect to the stars. The field of view of the telescope scans a great circle on the sky every ~ 2.4 hours and all objects brighter than $V \sim 18$ crossing the scan region may be detected. The telescope will image the area interior to Mercury but it gets no closer to the Sun than ~ 0.25 au. As Figure 1 shows, many of the objects in the outermost part of the belt are on eccentric orbits with aphelion $Q > 0.25$ au and so will spend some time in the scan region. Therefore, *Bepi-Colombo* may detect some objects belonging to the outer part of the Vulcanoid belt, although it will not image the bulk of the belt.

3 THE EARTH-MARS BELT

Let us now turn to the Earth-Mars belt. The high resolution simulation between 1.08 and 1.28 au exhibits a rich palette of dynamical behaviour. Figure 2 shows how the Earth-Mars belt has been sculpted by various mean motion and secular resonances. In the two lower panels, the filled circles show the instantaneous values at 100 Myr, while the crosses represent the maxima. For mean motion resonances, the upper panel indicates the semimajor axis of the resonance and order of the commensurability q . For the secular resonances, the upper panel shows the semimajor axis and inclination at which the effects of the two secular frequencies g_6 and s_6 are greatest. These linear secular resonances have been extracted from Michel & Froeschlé (1997) and Williams & Faulkner (1981). At the g_6 (or s_6) secular resonances, the averaged precession frequency of the asteroid's longitude of pericentre (or longitude of node) becomes equal to the sixth eigenfrequency of the planetary system, which is primarily due to Saturn.

The part of the belt between 1.08-1.117 au is populated with extremely stable test particles. This can be seen from the mean values of the instantaneous and maximum eccentricities ($\langle e_{\text{inst}} \rangle = 0.037$, $\langle e_{\text{max}} \rangle = 0.082$) and inclinations ($\langle i_{\text{inst}} \rangle = 1.81^\circ$ and $i_{\text{max}} = 4.86^\circ$). The gaps and the spikes

in eccentricity and inclination are in good agreement with the location of the mean motion resonances. However, from 1.17 au outwards, the presence of the linear secular resonances with Saturn tends to destabilize the orbits of the low inclination test particles. An island of stability between 1.208 to 1.214 au is able to avoid the disturbing effect of the secular resonances, thanks to the fact that most of the test particles' inclinations lie in the safety interval $1.8^\circ - 6.4^\circ$. Objects between 1.214 au and 1.28 au do not survive in this high resolution simulation. Nonetheless, Evans & Tabachnik (1999) found examples of some surviving test particles out to 1.28 au in their original 100 Myr integrations which covered the whole of the inner Solar system. We therefore take 1.28 au as the outermost edge of the Earth-Mars belt.

Conventionally speaking, the members of the Earth-Mars belt fall under the classification of Amor asteroids ($1.017 < q < 1.3$), which are part of the population of Near-Earth Objects (NEOs). Ground-based programs have found ~ 2000 NEOs, of which ~ 800 are Amors. The total number of NEOs is unknown. The present population is believed to have arisen from at least three sources, namely asteroids ejected from the Main Belt by the 3:1 mean motion resonance with Jupiter and the s_6 secular resonance; asteroids on Mars crossing orbits adjacent to the Main Belt; and defunct comets that have evolved from the Kuiper Belt through planetary encounters (e.g., Bottke et al. 2000). Ejected Main Belt asteroids and evolved comets are always planet-crossing and hence show large fluctuations in their eccentricity. For example, Gladman et al. (1997) show a number of dynamical tracks of asteroids ejected from the Main Belt and their evolution is almost always towards greater eccentricity. In one or two cases studied by Gladman et al., the evolution does pass through low eccentricity phases, but usually only for comparatively short periods of time. The probability of observing this part of the evolution is low. So, NEOs on nearly circular orbits are excellent candidates for being primordial. In other words, if the Earth-Mars belt of remnant planetesimals exists, an enhancement of asteroids on nearly circular orbits is expected in this region. Evans & Tabachnik (1999) carried out a search through Bowell's (1989) asteroidal orbital element database for objects between the semimajor axes of Earth and Mars which are not planet-crossing and with low inclinations and eccentricities. They found only three objects (1996 XB27, 1998 HG49 and 1998 KG3) among all the asteroids in the database. All three lie between 1.08 and 1.28 au. The success of ground-based surveys of NEOs in recent years has led to a substantial increase in available data, so it is worthwhile repeating the calculations. Using data from The Minor Planet Center, we searched for all objects between the semimajor axes of Earth and Mars which are not planet-crossing and which satisfy $i < 10^\circ$ and $e < 0.2$. The results are recorded in Table 1. There are twelve such objects known, of which nine lie in the suggested Earth-Mars belt. This tends to support the conjecture of Evans & Tabachnik (1999) that there is an enhancement of asteroids on nearly circular orbits in the belt.

Nonetheless, complex selection effects are present in the NEO dataset. To decide the issue, a catalogue of NEOs with a well-understood selection function is needed. Fortunately,

^{*} <http://www.vista.ac.uk>

[†] <http://sci.esa.int/home/bepicolombo/>

Name	q	Q	i	e	a	Discoverer
1989 ML	1.099	1.447	4.4°	0.137	1.273	Helin & Alu
1993 HA	1.094	1.463	7.7°	0.144	1.278	Spacewatch
1996 XB27	1.120	1.258	2.5°	0.058	1.189	Spacewatch
1998 HG49	1.065	1.335	4.42°	0.113	1.200	Spacewatch
1998 KG3	1.024	1.298	5.5°	0.118	1.161	Spacewatch
2000 AE205	1.004	1.322	4.5°	0.137	1.163	LINEAR
2001 KW18	1.046	1.439	7.2°	0.158	1.243	LONEOS
2001 SW169	1.184	1.313	3.6°	0.052	1.248	LINEAR
1993 KA	1.008	1.502	6.0°	0.197	1.255	LINEAR
1998 YB	1.222	1.420	6.8°	0.075	1.321	LONEOS
2001 AE2	1.239	1.460	1.7°	0.082	1.350	LINEAR
2001 QE96	1.274	1.347	7.3°	0.028	1.311	Spacewatch

Table 1. Data on all asteroids between the semimajor axes of the Earth and Mars with inclinations $i < 10^\circ$ and eccentricities $e < 0.2$ that are not planet-crossing. The object name, perihelion q , aphelion Q , inclination i , eccentricity e and semimajor axis a are given, as well as the discovery team. The upper nine asteroids lie in the Earth-Mars belt, the lower three do not. (The source of the data is The Minor Planet Center).

the ESA scanning satellite *GAIA* [‡] will provide exactly this. *GAIA* has three telescopes, ASTRO-1 and ASTRO-2 which perform astrometry and broad-band photometry, and SPECTRO which performs spectroscopy and medium-band photometry. *GAIA* can detect all objects brighter than $V \approx 20$. For the NEO population, Mignard (2002) shows that objects with absolute magnitude $H \lesssim 18$ will be observed at least two times in the ASTRO or the SPECTRO fields of view with the speed well-determined from the crossings. So, *GAIA* will provide a reasonably complete inventory of the NEO population with diameters of the order of a kilometre or larger.

4 CONCLUSIONS

Detailed maps of the fine-structure of two long-lived belts of stable orbits in the Solar system have been provided. This extends the results presented in Evans & Tabachnik (1999), which reported evidence that belts of remnant planetesimals could survive for the age of the Solar system. The Vulcanoid belt lies interior to the orbit of Mercury and extends from 0.09 to 0.20 astronomical units (au), though with a gaps at 0.15 and 0.18 au corresponding to a de-stabilising mean motion resonances with Mercury and Venus. Collisions drive evolution in the Vulcanoid belt and this proceeds slower at larger heliocentric distances. Searches should concentrate on the region between 0.16–0.18 au where kilometre-sized Vulcanoids are most likely to be found. The Earth-Mars belt between 1.08–1.17 au is an extremely stable zone. It is interrupted at 1.212 au due to the 3:4 commensurability with the Earth, while secular resonances with Saturn can pump up the eccentricities beyond 1.17 au. The belt may extend out to 1.28 au.

There are examples of stable orbits with small eccentricities and inclinations which are nonetheless depleted of bodies (in the outer Main Belt, for instance). The populations of small bodies of the solar system may have been dynamically excited or ejected by unknown processes during

the primordial evolution. So the belts are worth searching for because their presence or absence bears strongly on why the inner Solar system looks the way it does today. For example, substantial migration of Mercury would be strongly constrained by the discovery of a population of asteroids in the Vulcanoid belt.

ACKNOWLEDGMENTS

We thank Stephano Mottola for information on *Bepi-Colombo*. NWE is supported by the Royal Society.

REFERENCES

- Bottke W.F., Jedicke R., Morbidelli A., Petit J., Gladman B. 2000, *Science*, 288, 2190.
- Bowell E.G., 1999, The Asteroid Orbital Element Database, at <ftp://ftp.lowell.edu/pub/elgb/astorb.html>
- Campins H., Davis D.R., Weidenschilling S.J., Magee M. 1996, In “Completing the Inventory of the Solar System”, eds T.W. Rettig, J.M. Hahn, p. 85 (ASP Conference Series: San Francisco)
- Chapman C.R., 1987, In “The Evolution of Small Bodies in the Solar System”, eds M. Fulchignoni, L. Kresak, p. 79 (North Holland: Amsterdam)
- Durda D.D., Stern S.A., Colwell W.B., Parker J.W., Levison H.F., Hassler D.M. 2000, *Icarus*, 148, 312
- Evans N.W., Tabachnik S.A., 1999, *Nature*, 399, 41
- Gladman B., et al. 1997, *Science*, 277, 197
- Holman M.J., *Nature*, 387, 785
- Laskar J. 1997, *AA*, 317, L75
- Leake M.A., Chapman C.R., Weidenschilling S.J., Davis D.R., Greenberg R. 1987, *Icarus*, 71, 350
- Michel P., Froeschlé C. 1997, *Icarus*, 128, 230
- Mikkola S., Innanen K. 1995, *MNRAS*, 277, 497
- Mignard F. 2002, *AA*, submitted.
- Saha P., Tremaine S.D. 1994, *AJ*, 108, 1962
- Schumacher G., Gay J. 2001, *AA*, 368, 1108
- Stern S.A., Durda D.D. 2000, *Icarus*, 143, 360
- Vokrouhlický D., Farinella P., Bottke W.F. 2000, *Icarus*, 148, 147
- Weidenschilling S. 1978, *Icarus*, 35, 99
- Williams G.V., Faulkner J. 1981, *Icarus*, 46, 390

[‡] <http://astro.estec.esa.nl/gaia>